Journal of Rare Cardiovascular Diseases
ISSN: 2299-3711 (Print) | e-ISSN: 2300-5505 (Online)
www.jrcd.eu
RESEARCH ARTICLE

The Effect of Mesenchymal Stem Cells Derived Exosomes on Valproic Acid Induced Rat Model of Autism via Lnc RNA MALAT1 and its Target miRNA 125b through PI3K and PKB Pathway

Esraa Sameh Refaat[1], Marwa Mohamed Atef[2], Samia Abdelhamid Eldardiry[3], Ghada Ahmed Abdelaleem[4]

[1] Assistant Lecturer of Medical Biochemistry Department, Faculty of Medicine, Tanta University, Tanta, Egypt
[2] Assistant Professor of Medical Biochemistry Department, Faculty of Medicine, Tanta University, Tanta, Egypt
[3] Professor of Medical Biochemistry Department, Faculty of Medicine, Tanta University, Tanta, Egypt
[4] Professor of Medical Biochemistry Department, Faculty of Medicine, Tanta University, Tanta, Egypt

*Corresponding Author
Esraa Sameh Refaat

Article History
Received: 07.10.2025
Revised: 29.10.2025
Accepted: 19.11.2025
Published: 05.12.2025

Abstract: ***Background***: The present investigation was designed to assess the influence of exosomes derived from mesenchymal stem cells (MSCs) on a rodent model of autism that was induced by valproic acid. Unpredictable cognitive development is the primary characteristic feature of autism spectrum disorders (ASD), a collection of complex neurodevelopmental issues. ***Materials and methods:*** A total of 90 adult Wistar rats comprising 60 females and 30 males were kept in wire mesh cages under constant environmental conditions. The research involved the male off-springs only. 45 male Albino rat pups were allocated randomly into three equal groups (fifteen rats each): Group I (control), Group II: Autistic offspring of male Wistar rats received a standard diet and Group III: Autistic offspring of male Wistar rats received intravenous dose of Bone marrow-derived MSCs (BMSCs) derived exosomes. ***Results:*** Group II illustrated a highly significant reduction in metastasis associated lung adenocarcinoma transcript 1 (MALAT1) when compared to other groups (P-value $\leq$ 0.001). Group III demonstrated a statistically significant rise in MALAT1 gene expression when it was compared to other groups (P $\leq$ 0.001). A significant positive association has been observed among protein kinase B (PKB) and phosphoinositide 3-kinases (PI3K) (r 0.640), while a negative association has been detected among MALAT1 and microRNAs (miRNAs) 125b (r - 0.694), indicating a potential link between these factors. ***Conclusions:*** Treatment of autistic rats' model with exosomes, is responsible for regeneration of the damaged neuronal cells that results in expression of MALAT1 that lowers the micRNA 125b expression by its sponge-like effect.

Keywords: Mesenchymal Stem Cells Derived Exosomes, Valproic Acid, Lnc RNA MALAT1, miRNA 125b, Protein kinase B, Phosphoinositide 3-Kinases

INTRODUCTION

Autism spectrum disorders (ASD) are neurodevelopmental abnormalities, predominantly defined by abnormal cognitive progress, involving deficits in communication, language, repetitive behaviors, and restricted interests. [1] Although significant developments in neuropsychiatric genetics and the rising incidence of ASD, currently impacting one in fifty kids, the fundamental causes of its estimated ninety percent heritability mainly remain unknown. Zeidan and co-authors. [2] previous research has examined the connection between various gene expressions and polymorphisms in ASD patients to better understand its genetic basis. [3]

Noncoding RNAs, like long noncoding RNAs (lncRNAs) and microRNAs (miRNAs), have become integral regulators of gene expression. MicroRNAs are short, single-stranded RNAs that bind to the 3-untranslated region (3′-UTR) of the target messenger RNA. Degradation of the messenger RNA or translation inhibition are the outcomes of this action. [4]

LncRNAs, conversely, are endogenous RNA molecules longer than two hundred nucleotides that don't encode proteins. [5]

Emerging evidence suggests that miR-125b is a target gene of lnc-MALAT1, which has been shown to suppress cell proliferation, promote tau phosphorylation and apoptosis, and drive inflammation in neurological disorders. Overexpression of miR-125b can also enhance neuronal apoptosis, neuroinflammation, and oxidative stress, as seen in an in vitro Alzheimer's disease models [6]

This investigation aims to evaluate the impact of exosomes derived from mesenchymal stem cells (MSCs) on a rodent model induced by valproic acid.

MATERIAL AND METHODS

The study was an experimental one conducted at the Biochemistry Department, Faculty of Medicine, Tanta University, which took place between July 2023 and May 2024. The experimental animal model as well as all procedures for the experiment have been accepted by

the institutional "Research Ethics Committee, REC," Faculty of Medicine, Tanta University, Egypt (Approval Code 36264MD39/2/23).

Chemicals

Valproic acid: A white powder (1gm in a plastic ampoule, obtained from Sigma-Aldrich) has been dissolved in saline at a concentration of 1 gm/ 4 ml and subsequently supplemented via intraperitoneal injection (IP) in rat at a dosage of 400 mg per kg of body weight. [7]

Animals

Animal grouping and experimental design: The research was done in accordance with the declaration of Helsinki. A total of 90 adult Wistar rats, aged between 6 and 8 weeks and weighing 200-250 grams, consisting of 60 females and 30 males. The subjects have been housed in wire mesh cages under controlled atmospheric environment (25◦ C with alternating 12-hour day and night cycles) & given unlimited access to tap water ad libitum. Following a one-week acclimatization period, two females have been permitted to mate with a single male in the same cage. When the vaginal plug appear this marking the first day of gestation (GD1). Pregnant animals were randomly allocated into two sets according to the received treatment. Group A (control pregnant females): 20 pregnant rats received a single IP injection of 0.9% saline on the day 12.5 of the gestational day (GD 12.5). Group B (Valproic acid–treated pregnant females): 40 pregnant rats received a single IP injection of 400 mg/kg Valproic acid on the GD 12.5. The offspring were kept with their mothers till weaning (21 - 30 days). Experiments were conducted on the male offspring only. Figure 1

Methods

The current research has been performed on 45 male Albino rat pups (aged 21 days) after they were subjected to neurobehavioral assessment to separate the normal pups from the autistic pups including: Swimming performance test and T-maze test. The offsprings have been kept in wire mesh cages under constant environmental conditions (25 ◦ C and alternative day and night cycles of twelve hours each) and were allowed free access to food and tap water. After an initial acclimatization period, they have been allocated randomly into 3 equal groups (15 rat each). Figure 1

Group I (control group): includes healthy offspring of male Wistar rat received a standard diet.

Group II: Autistic offspring of male Wistar rat (treated by VPA) received a standard diet. Group III: Autistic offspring of male Wistar rats (treated by VPA) received IV dose of bone marrow MSCs obtained exosomes 1 × 107 MVs/rat (in rat tail) given once weekly for 3 successive weeks from the postnatal day 30st. [8]

At the finale of trial (one week following the last injected exosomes dose) behavioral tests were done to compare the three studied groups including: Swimming performance test and T-maze test were performed.

Swimming performance test:

The swimming test has been used to assess motor progress and reflex responses that function in an integrated and coordinated manner. A water-filled aquarium (28-29◦C) has been established to conduct the swimming test. Each animal has been permitted to swim in the aquarium, and their swimming has been monitored for ten seconds. The evaluation was done by observing the location of the nose and head in relation to the water's surface. The angle of swimming was categorized as follows: zero indicates that the head and nose are below the surface of the water, one indicates that the nose is under the surface, two indicates that the nose and top of the head are at or above the surface, but the ears are still below the surface, three indicates that the waterline reaches the mid-ear level, and four indicates that the waterline is at the bottom of the ears, similar to the third category. The test pups were dried and returned to their cages following the observation. [9]

T-maze test: The T-maze has been utilized to assess repeated and limited behaviors. Typical rats rotate among arms based on their memory, indicating their motivation for environmental exploration. Five sessions have been done for each rat, and the optimal choice has been assessed. [10] The T maze is a wooden structure that is oriented in the form of a horizontal T. It includes a start alley that is thirty cm in length and ten cm in breadth, as well as a goal arm that is also thirty cm in length and ten cm in width. The wall height is 20 cm. [11] The rat has been positioned in the examination room for ten minutes, after which they have been positioned in the start zone and let to select the goal arm. The rat has been restricted to the selected arm for thirty seconds, thereafter removed, and placed in the home cage for sixty seconds. Subsequently, it has been returned to the start arm to initiate the second trial. The trial has been done five consecutive times, with a one-minute interval among each and a thirty-second habituation period in the selected arm. The percentage of alternation among the left and right arms has been evaluated. [10]

At the conclusion of the trial (one week following the final administration of exosomes), all animals have been sacrificed under anesthesia, and samples of brain tissue have been procured and analyzed. Ultimately, sacrificed rats have been securely gathered in a designated container in accordance with safety protocols and infection control procedures, and sent alongside hospital biohazards.

Animals in the three groups studied were subjected to the following: The histopathological examination of brain tissue specimens pertaining to all groups, estimation of PI3K and PKB concentration, in the brain tissues by ELISA technique, and molecular

investigations: LncRNA MALAT1 and miR-125b gene expression in the brain tissues by qRT-PCR

Preparation, isolation & detection of BM-MSCs in culture:

MSCs have been isolated from 5 white albino rat bone marrow. Inside a Class II laminar flow biosafety cabinet, the bones were washed twice with PBS containing 1% penicillin-streptomycin to eliminate blood and tissue debris. The bones were then moved to a new 100-mm culture dish with 5 mL fresh Dulbecco's Modified Eagle Medium (DMEM).The epiphyseal ends were trimmed, the bone marrow was flushed by 5 mL DMEM until the marrow was fully removed and the bones became visibly pale. After flushing, flushed bone marrow content was filtered through a 70-mm filter mesh, washed, and resuspended with 7 ml Complete DMEM media (high glucose) supplemented with 10% Fetal Bovine Serum (FBS), 1% penicillin and streptomycin in 25 ml culture flask. The flask was then incubated at 37C in a 5% CO2 incubator.

Cultured MSCs have been evaluated by their morphology by using inverted microscopes (spindle fusiform fibroblast like cells), adhesion properties and fluorescence-activated cell sorting (FACS). [12] Upon achieving a confluence rate of 85-90%, cultures have been rinsed twice with PBS, and cells have been subjected to trypsinization using 0.25% trypsin in 1mM EDTA. Following centrifugation, cell pellets have been re-suspended in serum-supplemented media and cultured in a 50 cm culture flask. The resultant cultures have been designated as 1st -passage cultures. [13]

Phenotypic fluorescence-activated cell sorting (FACS)
Fluorescence-activated cell sorting (FACS) is a widely utilized tool for analyzing the chemical & physical characteristics of specific cells in suspension. It uses light scattering properties of vesicles to sort individual cell populations using fluorescently labeled antibodies. Flow cytometry detects particles suspended in fluids by their interaction with a laser beam. This method has been utilized to evaluate the immune profile of MSC, utilizing the International Society for Cellular Therapy standard. The cells were collected, centrifuged, washed, and incubated with antibodies. Flow cytometric analysis of the cultured MSCs surface markers will be done by immunostaining with monoclonal antibodies against cluster differentiation 90 (CD 90) as a positive marker and CD 45 (hematopoietic markers) as a negative marker for MSCs. [14]

Isolation, identification and quantitation of exosomes derived from Bone marrow MSCs; Exosomes have been isolated from MSCs cultured media by ultracentrifugation. [8]

Identification, Characterization and Quantification of exosomes derived from BM-MSCs [15]
Exosome size distribution:

Exosomes size distribution was determined using a Nanosight NS300 particle size analyzer (NTA; Malvern Panalytical, Malvern, UK). Exosomes were characterized by their sizes that ranged from 30-150 nm. (16).

The total protein concentration of exosomes has been revealed utilizing the Bradford protein assay
FACS for CD81 and CD63: CD81 and CD63 have elevated expression levels in exosomes compared to MSCs. [17] Saturating concentrations (1:100 dilution) of fluorescein isothiocyanate-conjugated-human monoclonal antibodies: anti-CD63 (ab18235) and anti-CD81 (BD Pharmingen) were added to phosphate-buffered saline enriched with three percent fetal bovine serum (FBS). Exosomes were collected and resuspended in this solution. Samples have been analyzed via forward scatter analysis (Becton-Dickinson, Canada).

Injection of prepared exosomes in rats of group III: The research involved the autistic rat's group III; they received intravenous doses of BM-MSCs-derived exosomes once weekly for three weeks. [8] After anesthesia, rats were sacrificed & brain tissue specimens were collected for biochemical, histological, and genetic studies.

Tissue sampling

Following scarification, brain tissues have been meticulously dissected, weighed, & rinsed thrice with ice-cold saline to eliminate extraneous materials, then separately blotted on ash-free filter paper. The brain has been chilled on ice and divided and subjected to the following: the 1st part of brain tissues was formalin-fixed (10%) and processed. paraffin sections have been stained with Haematoxylin & Eosin & photomicrographs have been taken at different magnification power for histopathological assessment of tissue specimens. 2nd part of brain tissues has been wrapped in foil of aluminium & stored at – 80 C° till used for preparation of tissue homogenates for total protein assay, ELISA, and qRT-PCR.

Histopathological examination

Formalin-fixed brain tissues have been treated, and five micrometers thick paraffin slices have been stained with hematoxylin & eosin (H&E), followed by the acquisition of photomicrographs at various magnifications.

Preparation of cerebral tissue homogenates:

Preparation of brain tissue homogenates for the assessment of protein kinase B (PKB) and phosphoinositide 3-kinases (PI3K) levels. A 1:5 weight-to-volume ratio was used to weigh and homogenize the brain tissue samples in 10 mM cold potassium phosphate buffer saline at pH 7.4. The Potter-Elvehjem tissue homogenizer was employed for this purpose, 20 to 30 upward and downward strokes were employed in

the technique. At 4°C, the crude homogenate was subjected to a 20-minute centrifugation at 300 revolutions per minute. Prior to its utilization, the supernatant has been segregated and stored at -80◦C.

Preparation of phosphate buffer saline (PBS) (10mM, pH 7.4):
Solution A: Potassium dihydrogen orthophosphate 10 mM (MW: 136.1) was prepared by dissolving 1.361g of potassium dihydrogen orthophosphate in one liter of normal saline. Solution B: Dipotassium hydrogen phosphate 10 mM (MW: 174.18) was prepared by dissolving 1.7418 g of dipotassium hydrogen phosphate in one liter of normal saline. Then 198 ml of solution A were added to 802 milliliters of solution B, to prepare one liter of 10mM phosphate buffer saline with adjustment of pH to 7.4.

Estimation of protein content in tissue homogenates and exosomes: The protein content of tissue homogenates and exosomes was quantified by Bradford method (BioRad, Hercules, CA, USA) Ma, 2020 #18}. The spectrophotometer has been set at 595 nm.

Determination of PKB level in brain tissue homogenates (ng/mg protein): The level of PKB in brain tissue homogenate was determined by an enzyme-linked immune-sorbent assay utilizing a commercially available kit (Catalogue number #: 201-11-0202) supplied by Sunred Biotechnology Co., Shanghai, China.

Determination of PI3K of studied rats' groups (ng/mg protein): Using commercial rat PI3K ELISA kit supplied by Sunred Biological Technology Co., Ltd, Shanghai. China. Catalogue No (201-11-0439).
Quantitative Real time PCR amplification for cDNA of the house keeping gene Glyceraldehyde 3-phosphate dehydrogenase (GAPDH) and MALAT1 genes

Quantitative real-time PCR (qRT-PCR) was performed using the Applied Biosystems StepOnePlus™ Real-Time PCR System (Model No. 4376592, Thermo Fisher Scientific, USA). qRT-PCR with SYBR Green was used to measure the expression of long non-coding RNAs of MALAT1 in brain tissue with GAPDH as an internal reference. PCR reagents: The isolated cDNA was amplified using TOP real™ qPCR 2X PreMIX (SYBR Green with low ROX) kit from enzynomics, Munji-ro,Daejeon,Korea, K0221 and gene specific primers obtained from Thermo Fisher Scientific,
Waltham, Massachusetts, United State of America. Table 1
Reactions were carried out in a total volume of 25 µL, containing SYBR Green Master Mix, 1 µM of each primer, and 5 µL of cDNA template. All reactions were performed in triplicate to ensure reproducibility. Positive and negative controls were included in each run to validate the accuracy and specificity of amplification: A positive control consisting of a template cDNA (target gene sequence) was used to confirm the performance of the reagents and amplification efficiency. A no-template control (NTC) containing all reaction components except the cDNA template was included to monitor possible contamination or primer-dimer formation.

Additionally, a no-reverse transcriptase (NRT) control was run to confirm the absence of genomic DNA contamination in RNA samples. Amplification plots were examined for each control reaction, Only assays showing no amplification in negative controls and consistent amplification in positive controls were accepted for analysis and any run showing amplification in the NTC or NRT was excluded and repeated. The inclusion of internal positive and negative controls in each qRT-PCR run confirmed assay reliability and eliminated potential artifacts due to contamination or non-specific amplification. Housekeeping Gene: Expression levels were normalized to GAPDH as an internal reference gene to account for variation in RNA input and reverse transcription efficiency.

For Data Validation, the specificity of amplification was verified by melting curve analysis of selected amplicons. Ct values with a standard deviation > 0.5 between triplicates were excluded from analysis.

For miR-125b gene expression
The TransScript® Green miRNAs Two-Step Quantitative Real-time PCR SuperMix kit has been utilized for the reverse transcription of specific miRNAs and quantitative RT-PCR. Catalog Number AQ202-01 has been acquired from Transgen Biotech [16]. The TransScript® Green miRNAs 2-Step Quantitative Real-time PCR SuperMix is a kit including the TransScript® miRNAs RT Enzyme Mix, 2×TS miRNAs Reaction Mix, & Perfect Start TM Green qPCR Super Mix, designed for the identification and quantification of miRNAs from total RNA, small RNA, or other sources. Procedures: First strand DNA synthesis: Reaction components for miRNA cDNA Synthesis (Total RNA 5 µl, TransScript® miRNA RT Enzyme Mix 1 µl, 2×TS miRNA Reaction Mix 10 µl, RNase-free Water 4 µl) the mix has been incubated at 37◦C for one hour. Then it was incubated at 85% for 5 seconds to inactivate the RT enzyme mix. The primers used are shown in Table 2. These primers are based on published rat sequences and were checked by BLAST.
Calculation of relative quantification (RQ) (relative expression)

After the RT-PCR process, the data has been represented as Cycle Threshold (Ct). The PCR data sheet included the Ct values for the housekeeping gene (RNU6B) and the evaluated gene (miRNA 125b). The utilization of a control sample is necessary in order to evaluate the expression of a particular gene. By computing the delta-delta Ct (ΔΔCt), the relative

quantification of each target gene is determined. The RQ of each gene has been calculated by taking 2-ΔΔCt. For miRNA, the kit provided the universal reverse primer.

Statistical analysis

The statistical presentation and analysis of the current research results have been performed, with data expressed as mean ± SD or as counts and percentages. The ANOVA and Tukey tests have been done utilizing the SPSS V.20 software. A p-value of fewer than 0.05 was deemed significant.

RESULTS

MSCs have been recognized through their morphological fibroblast spindle shape. Figure 2(a,b) . MSCs are negative for surface indicator CD45 (1.84 %), but positive for CD90 (98.16 %). (Figure 3).

MSCs derived exosomes characterization by FACS: MSCs derived exosomes show a positive finding for surface indicator CD63 & CD81, which are characteristic for exosomes. (Figure 4)

Histopathological results of the studied groups:

The research examined brain specimens from control and diseased groups. Control groups had normal cerebral cortex, neurons, pyramidal cells, and a normal hippocampus with dentate gyrus. The cerebellum showed normal purkinje cell layer and granular layer. In contrast, diseased groups showed hemorrhage, congestion, and gliosis, with a pyknotic shrunken nucleus and decreased purkinje cell count. Exosome-treated groups had normal pyramidal cells, few congested blood vessels, and some cerebral edema. The hippocampus and cerebellum showed normal granular and molecular layers. Figure 5,6.

A highly statistically significant variation in the values of PI3K and PKB has been observed among all groups (P< 0.001). In contrast to the other groups, Group II demonstrated a significant increase in PI3K and PKB levels, while Group III demonstrated a statistically significant decrease in PI3K and PKB levels when compared to Group II (P<0.001). Nevertheless, there was no significant difference in PI3K and PKB levels between Group I and Group III. Table 3

The Tukey post-hoc test demonstrated that group II experienced a significant decrease in its angle of swimming score and percentage of alteration when compared to the other groups (P<0.001). Conversely, group III experienced an increase in its angle of swimming score and percentage of alteration when compared to group II (P<0.001). Table 4

A highly significant variations have been observed in MALAT1 gene expression and miRNA-125b among all groups (P< 0.001). Table 5

In group II and III,, there was a significant positive association between PKB & PI3K (r 0.640). Also, a significant negative association has been observed among MALAT1 and miRNA 125b (r - 0.694). Table 6

Table 1: The primers utilized for quantitative real-time polymerase chain reaction

Gene	Primer sequence from 5′- 3′	Accession no.
LncRNA-MALAT1	5′- CAGACCACCACAGGT TTACAG-3′	NR_002847.3
	5′-AGACCATCCCAAAATG CTTCA-3′	
GAPDH	5′-TGACTTCAACAGCGA CACCCA-3′	NM_001411843.1
	5′-CACCCTGTTGCTGTAGC CAAA-3′	

Table 2: The primers used for quantitative real-time polymerase chain reaction

Gene	Primer sequence from 5′- 3′	Accession no.
miRNA- 125b	F: 5′-ACGGGTTAGGCTCTTGG -3′	MI_0000446.
	R: 5′-CAGTGCGTGTCGTGGAGT-3′	
RN U6B	F: 5′-GCTTCGGCAGCACATATACTAAAAT-3′	NG_044085.2
	R: 5′-CGCTTCACGAATTTGCGTGTCAT-3′	

Table 3: Comparative analysis among the three examined groups according to PI3K and PKB level concentration

	PI3K (ng/mg ptn)	F	P
Group I (n = 15)	0.384 ± 0.207		
Group II (n = 15)	1.595 ± 0.567	47.307*	<0.001*
Group III (n = 15)	0.608 ± 0.176		
Tukey's test	P1<0.001*, P2=0.221, P3<0.001*		
	PKB (ng/mg ptn)		
Group I (n = 15)	0.431 ± 0.308		
Group II (n = 15)	1.280 ± 0.471	24.591*	<0.001*
Group III (n = 15)	0.595 ± 0.233		

Tukey's test	P1<0.001*, P2=0.418, P3<0.001*		

Data are presented as mean ± SD. *: Statistically significant at p ≤ 0.05, P1: significance bet. group I and II, P 2: significance bet. Group I and III, P3: significance bet. group II and III, F: F for One way ANOVA test, Group I: Control group, Group II: Diseased group, Group III: (BM-MSC) derived exosomes treated group, PKB: Protein kinase B, PI3K: Phosphoinositide 3-kinases.

Table 4: Comparative analysis among the three examined groups according to swimming performance test and T-maze test

	Swimming performance test (meaning angle swimming score)	F	P
	A = (At 30th day of pup's life)		
Group I (n=15)	3.0 – 4.0	51.924*	<0.001*
Group II[T] (n=30)	2.09 – 3.11		
	B = (By the end of the experiment)		
Group I (n = 15)	3.87 ± 0.35		
Group II (n = 15)	2.27 ± 0.46	53.444*	<0.001*
Group III (n = 15)	3.53 ± 0.52		
Tukey's test	P1<0.001*, P2=0.115, P3<0.001*		
	T-maze test (percentage of alternation %)		
	A = (At 30th day of pup's life)		
Group I (n=15)	89.20 ± 5.23	485.065*	<0.001*
Group II[T] (n=30)	40.1 ± 5.35		
	B = (By the end of the experiment)		
Group I (n = 15)	89.20 ± 5.23		
Group II (n = 15)	38.0 ± 5.35	455.065*	<0.001*
Group III (n = 15)	76.27 ± 3.77		
Tukey's test	P1<0.001*, P2<0.001*, P3<0.001*		

Data are presented as mean ± SD. *: Statistically significant at p ≤ 0.05, P1: significance bet. group I and II, P 2: significance bet. Group I and III, P3: significance bet. group II and III, F: F for One way ANOVA test, Group I: Control group, Group II: Diseased group, Group III: (BM-MSC) derived exosomes treated group.

Table 5: Comparative analysis among the three examined groups regarding MALAT1 gene expression and miRNA-125b

	MALAT1 (fold change)	F	P
Group I (n = 15)	1.03 ± 0.10		
Group II (n = 15)	0.11 ± 0.05	437.234*	<0.001*
Group III (n = 15)	3.50 ± 0.55		
Tukey's test	P1<0.001*, P2<0.001*, P3<0.001*		
	miRNA-125b (fold change)		
Group I (n = 15)	1.01 ± 0.05		
Group II (n = 15)	2.21 ± 0.40	61.664*	<0.001*
Group III (n = 15)	1.29 ± 0.35		
Tukey's test	P1<0.001*, P2=0.047*, P3<0.001*		

Data are presented as mean ± SD. *: Statistically significant at p ≤ 0.05, P1: significance bet. group I and II, P 2: significance bet. Group I and III, P3: significance bet. group II and III, F: F for One way ANOVA test, Group I: Control group, Group II: Diseased group, Group III: (BM-MSC) derived exosomes treated group.

Table 6: Correlation among different parameters in group II and III

		PI3K (ng/mg ptn)	PKB (ng/mg ptn)	Swimming performance test	T-maze test	MALAT1 (fold change)	miRNA-125b (fold change)
				Group II			
PI3K (ng/mg ptn)	r	1.000	0.640	0.025	0.001	-0.469	0.108
	p	--	**0.010***	0.929	0.998	0.078	0.701
PKB (ng/mg ptn)	r	--	--	0.482	0.359	-0.386	0.232
	p	--	--	0.069	0.189	0.155	0.405
Swimming performance test	r	--	--	--	0.409	-0.334	0.618
	p	--	--	--	0.130	0.223	0.014
T-maze test	r	--	--	--	--	-0.228	0.225
	p	--	--	--	--	0.414	0.419
MALAT1 (fold change)	r	--	--	--	--	--	-0.694
	p	--	--	--	--	--	**0.004***
miRNA-125b (fold change)	r	--	--	--	--	--	--
	p	--	--	--	--	--	--
				Group III			
PI3K (ng/mg ptn)	r	1.000	0.688	-0.233	-0.130	-0.396	0.221
	p	--	**0.005***	0.403	0.644	0.144	0.428
PKB (ng/mg ptn)	r	--	--	-0.103	-0.201	0.032	-0.157
	p	--	--	0.715	0.472	0.910	0.575
Swimming performance test	r	--	--	--	0.068	-0.210	-0.210
	p	--	--	--	0.808	0.452	0.425
T-maze test	r	--	--	--	--	0.077	0.077
	p	--	--	--	--	0.784	0.784
MALAT1 (fold change)	r	--	--	--	--	--	-0.541
	p	--	--	--	--	--	**0.037***
miRNA-125b (fold change)	r	--	--	--	--	--	--
	p	--	--	--	--	--	--

r: Pearson coefficient. *: Statistically significant at $p \leq 0.05$, PKB: Protein kinase B PI3K: Phosphoinositide 3-kinases.

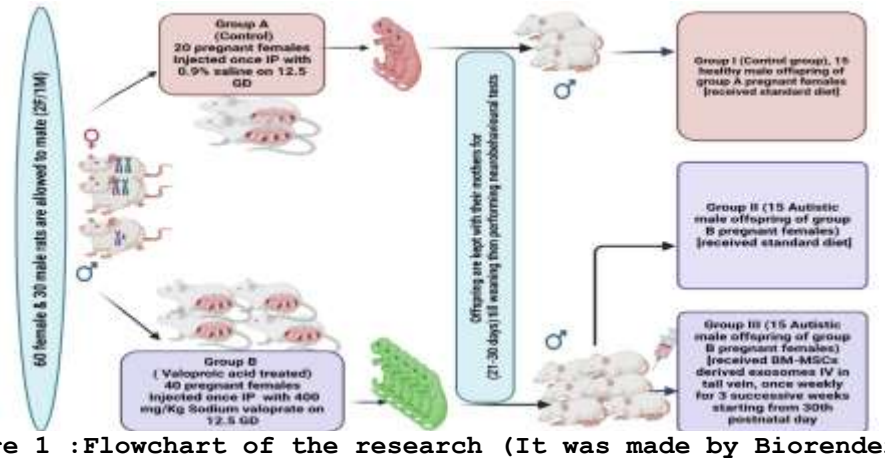

Figure 1 :Flowchart of the research (It was made by Biorender).

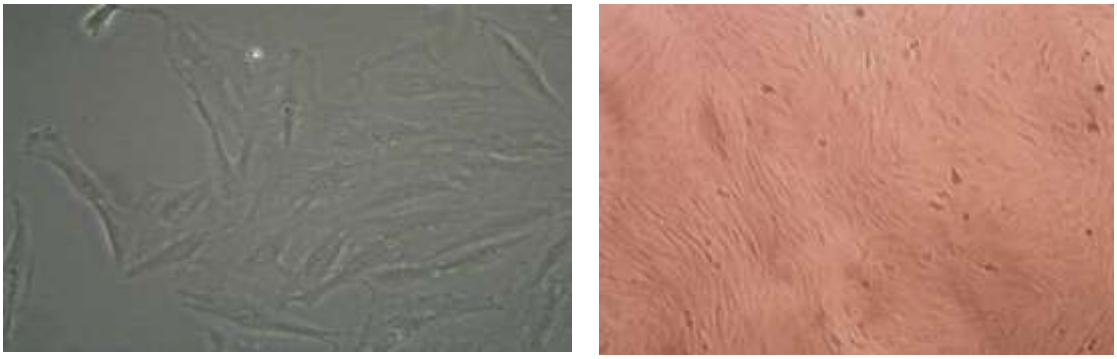

(a)Spindle fusiform fibroblast like MSCs (3rd day of cell culture). (b)Mesenchymal stem cells with confluency (80%-90%).

Figure 2: BM MSCS identification by inverted microscope

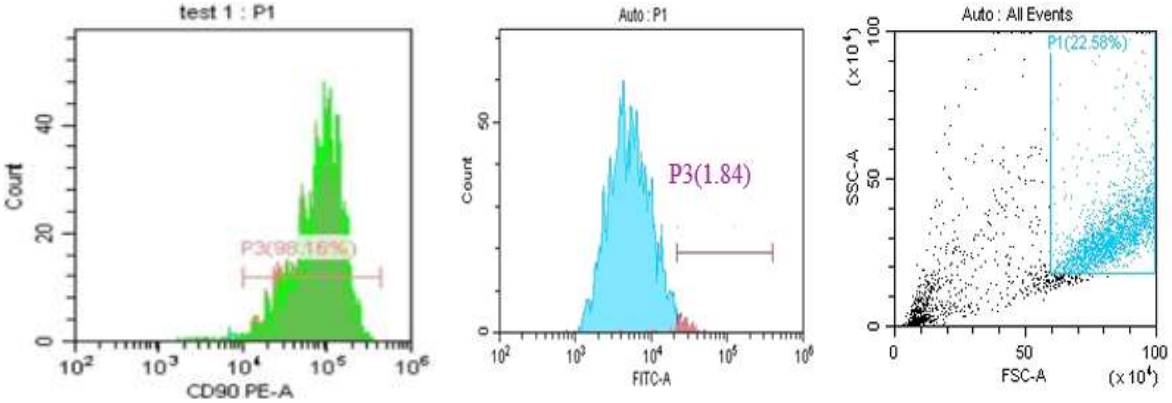

Figure 3: MSCs flow cytometric analysis for CD45 and CD90..

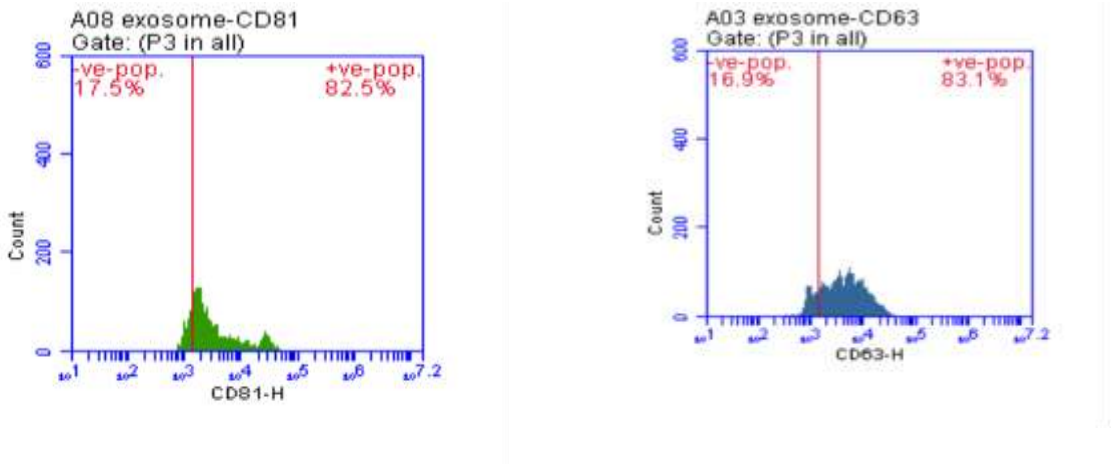

Figure 4: BM.MSCs derived exosomes characterization by FACS.

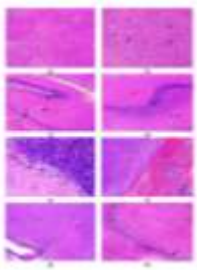

Figure 5: Histopathological examination of studied groups

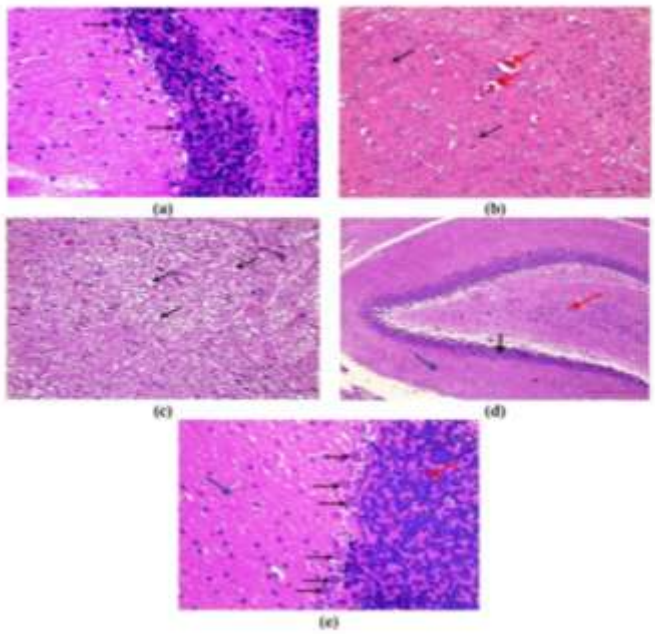

Figure 6: Histopathological examination of studied groups

Figure legends:

Figure 1: Flow chart of experimental design.
Figure 2: (a) Spindle fusiform fibroblast like MSCs and (b) mesenchymal stem cells with confluency more than 80%.
Figure 3: MSCs flow cytometric analysis and
Figure (4); BM-MSCs derived exosomes characterization.
Figure 5: Micrograph of H&E stained section in (a) normal cerebral cortex of control group (group I) showing normal neurons (H. & E. 100x) scale bar 80 µm, (b) cerebral cortex with normal pyramidal cells [black arrows] in control group (group I) (H. & E. x200) scale bar 40 µm, (c) normal hippocampus in control group showing dentate gyrus with inner hilar pyramidal cells [red arrow], middle granule cell layer [black arrows], and outer molecular layer [blue arrow] (x100) scale bar 80 µm, (d) normal dentate gyrus with inner hilar pyramidal cells [red arrow], middle granule cell layer [black arrow], and outer molecular layer [blue arrow] (x200) scale bar 40 µm, (e) normal cerebellum in control group showing normal purkinje cell layer with average number [black arrows], granular layer [red arrow], and molecular layer [blue arrow] (x400) scale bar 25 µm, (f) cerebral cortex of the diseased group (group II) showing hemorrhage and congestion [black arrows] (x100) scale bar 80 µm, (g) cerebral cortex of the diseased group (group II) showing hemorrhage [black arrow] and gliosis [red arrow] (x100) scale bar 80 µm, (h) hippocampus in the diseased group (group II) showing pyknotic shrunken nucleus of the granule cell layer [black arrow] (x200) scale bar 40 µm.

Figure 6: Micrograph of H&E stained section in (a) the cerebellum of the diseased group (group II) showing decreased number of purkinje cells, compared to control group [black arrows] (x400) scale bar 25 µm , (b) cerebral cortex of the treated group (group III) showing normal pyramidal cells [black arrows] together with few congested blood vessels [red arrows] (x200) scale bar 40 µm, (c) the cerebral cortex of the treated group (group III) showing cerebral edema [black arrows] (x200) scale bar 40 µm , (d) hippocampus of the treated group (group III) showing normal dentate gyrus with inner pyramidal cells [red arrow], middle granule cell layer [black arrow], and outer molecular layer [blue arrow] (x100) scale bar 80 µm and (e) cerebellum of the treated group (group III) showing purkinje cell layer with average number [black arrows], granular layer [red arrow], and molecular layer [blue arrow] (x400) scale bar 25 µm.

DISCUSSION

Valproic acid (VPA), a widely used antiepileptic and mood-stabilizing drug, is utilized in animal models to induce autism spectrum disorder (ASD) due to its epigenetic impact—particularly via inhibition of histone deacetylase (HDAC), affecting neurotransmission and gene expression.(18)

Our information discovered an obvious decline in neurobehavioral aspects that were assessed by swimming performance test and T-maze spontaneous alternation test, after VPA injection and manifested by impaired motor coordination and impaired memory.

The T-maze has been utilized to assess repetitive and limited behaviors. The percentage of alternation among

the left & right arms has been evaluated. Typical rats rotate among arms based on their memory, indicating their motivation for environmental exploration. The autistic rat had a reduced percentage of change, indicating repetitive activity. This aligns with Cezar and co-authors. [10] indicated that animals that persistently return to the same spatial place in one arm of the T-maze are classified as exhibiting an "autistic type." A swimming performance assessment was done to measure motor progress & reflex responses that operate in a synchronized and integrated fashion. All animals were permitted to swim at the aquarium center, and the swimming activity was monitored for ten seconds. The swimming performance has been evaluated based on the position of the head and nose (angle) relative to the surface of water. Thereafter, the test pups were dehydrated and placed back in their cages. [9] The autistic rats showed highly significant decrease in the angle of swimming score when it was compared to other groups. This runs in accordance with Schneider and Przewłocki and co-authors. [19] measured behavioral changes in rat prenatally exposed to valproic acid.

The histopathological results of the present research revealed hemorrhage and congestion and gliosis in cerebral cortex, pyknotic shrunken nucleus of the granule cell layer in the hippocampus and decreased number of Purkinje cells, compared to control group in the cerebellum of group II.

The PI3K-AKT/mTOR signaling pathway significantly influences neurons, serving as a conduit for the regulation of various cellular processes associated with autism. Growing data indicates that this pathway is significantly dysregulated in autism and several neurodegenerative illnesses.

In contrast to the control groups, those with autism showed significantly higher PI3K-AKT levels in the current investigation. Axonal dysregulation, megalencephaly, alterations in protein synthesis, neuron size, cerebral cell proliferation, and neuronal circuit connectivity across different brain regions are all linked to the upregulation of the PI3K-AKT/mTOR signaling pathway, which occurs when the upstream negative regulator PTEN is inactivated. The PI3K-AKT/mTOR signaling pathway is an important regulatory network that affects certain physiological features of autism. [20]

From an alternative perspective, LncRNAs have been identified as playing a role in several diseases. LncRNAs are RNA transcripts exceeding two hundred nucleotides that don't contain proteins, influencing mRNA expression at genomic loci and regulating mRNA breakdown post-transcriptionally. [21]

The current research revealed a significant reduction in MALAT1 levels in the autistic group in comparison to other groups, as MALAT1 is upregulated throughout neural as well as glial differentiation, processes essential for branching, neuronal growth, and the proliferation of GABA interneurons. In nuclear loci associated with complex assembly, it regulates the alternative splicing of genes and transcription factors to regulate synapse development in mature neurons. Dysregulation in MALAT1 can impair synaptic function. [22]

The current research revealed a considerable elevation of miRNA 125b in the autistic group compared to other groups. Synaptic transmission was reduced as a consequence of the upregulation of miRNA-125b, which led to the formation of elongated and slender spines. This was evident in the presence of these spines. Subsequently, it was determined that miRNA-125b targets the NR2A component of the N-methyl-D-aspartate receptor, which influences memory consolidation and synaptic plasticity. [23]

MiRNA 125b inhibit ectodermal (CNS-related) and endodermal differentiation in embryonic stem cells without affecting mesoderm or cell proliferation, impair neuronal development when overexpressed and promote astrogliosis and induce cell cycle defects seen in neurodegeneration.(24)

MiR-125b binds to the 3'UTRs of PTEN mRNA, leading to: Decreased PTEN mRNA stability, reduced PTEN protein expression. This results in upregulation of the PI3K/AKT pathway, promoting excessive proliferation, abnormal numbers of neurons, glial cells, dendrites, or spines, deficits in synaptic growth and plasticity, dysmorphic dendritic spines and disrupted synaptic protein homeostasis.(25)

PTEN downregulates the PI3K/AKT/mTOR pathway by converting PIP3 to PIP2, thus limiting AKT signaling. Mutations in PTEN lead to overactivation of this pathway, contributing to ASD behaviors.(26)

MALAT1 and miRNA 125b were found to have a significant negative correlation in existing research. Corroboration of this conclusion is provided by J. Zhuang and co-authors. [27] stated that lnc-MALAT1 levels in CSF and plasma have been downregulated, whereas miR-125b levels in cerebrospinal fluid and plasma have been upregulated in Alzheimer's disease cases to PD patients and controls. This distinction effectively differentiates AD cases from PD cases and controls, with CSF/plasma lnc-MALAT1 negatively correlating with miR-125b.

The focus of stem cell research is a variety of maladies, with a particular emphasis on neurological diseases. A prospective source for stem cell-based therapies, MSCs possess immunomodulatory properties, pro-angiogenic attributes, and the capacity to differentiate into numerous lineages. [28] MSCs can be readily extracted

from diverse sources like adipose tissue, Wharton's Jelly from umbilical cords, bone marrow, and dental pulp, prompting extensive research into their application in cell transplantation strategies for PD. [29] MSCs play a crucial role in tissue homeostasis and can influence cellular activity via direct cell-to-cell contacts or by releasing soluble biological mediators, including exosomes.

In this research, Rats in group III: Autistic male offsprings of (group B= treated by VPA) female Wistar rats were received intravenous dose of Bone marrow-derived MSCs (BM-MSC) derived exosomes 1×107 MVs/rat (in rat tail) given once weekly for three successive weeks starting from the 30th post-natal day.
In this current research, rats received BM-MSCs derived exosomes exhibited significant reduction in PI3K _PKB pathway compared to autistic group, in addition, rats received BM-MSCs derived exosomes group III exhibited significant rise in MALAT1 compared to other groups and significant reduction in miRNA 125b compared to other groups
Our histological results demonstrated that treatment with MSCs derived exosomes group III showed normal pyramidal cells together with few congested blood vessels, there was some cerebral edema in cerebral cortex, the hippocampus showed normal dentate gyrus with inner pyramidal cells, middle granule cell layer, and outer molecular layer, The cerebellum showed purkinje cell layer with average number, granular layer, and molecular layer. A significant difference was found between the BM MSCs derived exosomes group III and autistic group II, suggesting that BM-MSCs derived exosomes had a regenerative effect.

Patel and co-authors. [30] The research demonstrated that exosomes migrate to the spleen within one hour of administration and subsequently reach the brain several hours after TBI. In rats that were administered exosomes following TBI, there was a significant improvement in motor function and a reduction in cortical brain injury. The significance of MALAT1 in exosome-mediated recovery was underscored by the minimal regenerative impacts of therapy with exosomes lacking MALAT1 or conditioned medium devoid of exosomes. Analysis of the RNA sequence of the brain and spleen revealed that MALAT1 controls pathways associated with inflammation, cell cycle, apoptosis, and regenerative molecular processes. Our findings imply that MALAT1 controls the synthesis of snoRNAs and other noncoding RNAs.

CONCLUSION

Treatment of autistic rats' model with exosomes, is responsible for reprogramming and regeneration of the damaged neuronal cells that results in expression of MALAT1 that lowers the micRNA 125b expression by its sponge-like effect. This leads to decrease PI3K-PKB level, those that are strongly sharing in flaring of ASD symptoms and signs, marked improvement of the motor and behavioral manifestations of ASD have been achieved.

REFERENCES

1. Quartier A, Chatrousse L, Redin C, Keime C, Haumesser N, Maglott-Roth A, et al. Genes and pathways regulated by androgens in human neural cells, potential candidates for the male excess in autism spectrum disorder. Biol Psychiatry. 2018;84:239-52.
2. Zeidán-Chuliá F, de Oliveira B-HN, Casanova MF, Casanova EL, Noda M, Salmina AB, et al. Up-regulation of oligodendrocyte lineage markers in the cerebellum of autistic patients: evidence from network analysis of gene expression. Molecular neurobiol. 2016;53:4019-25.
3. Noroozi R, Taheri M, Ghafouri-Fard S, Bidel Z, Omrani MD, Moghaddam AS, et al. Meta-analysis of GABRB3 gene polymorphisms and susceptibility to autism spectrum disorder. J Mol Neurosci. 2018;65:432-7.
4. Hrdlickova B, de Almeida RC, Borek Z, Withoff S. Genetic variation in the non-coding genome: Involvement of micro-RNAs and long non-coding RNAs in disease. Biochim Biophys Acta. 2014;1842:1910-22.
5. Statello L, Guo CJ, Chen LL, Huarte M. Gene regulation by long non-coding RNAs and its biological functions. Nat Rev Mol Cell Biol. 2021;22:96-118.
6. Zhuang J, Cai P, Chen Z, Yang Q, Chen X, Wang X, et al. Long noncoding RNA MALAT1 and its target microRNA-125b are potential biomarkers for Alzheimer's disease management via interactions with FOXQ1, PTGS2 and CDK5. Am J Transl Res. 2020 Sep 15;12(9):5940-5954. PMID: 33042470; PMCID: PMC7540111.
7. Zhou J, Cao Y, Wang X, Li P, Xu W. Deep recurrent models with fast-forward connections for neural machine translation. Nat Rev Mol Cell Biol. 2016;4:371-83.
8. Bruno S, Grange C, Deregibus MC, Calogero RA, Saviozzi S, Collino F, et al. Mesenchymal stem cell-derived microvesicles protect against acute tubular injury. J Am Soc Nephrol. 2009;20:1053-67.
9. Schapiro S, Salas M, Vukovich K. Hormonal effects on ontogeny of swimming ability in the rat: assessment of central nervous system development. Science. 1970;168:147-50.
10. Cezar LC, Kirsten TB, da Fonseca CCN, de Lima APN, Bernardi MM, Felicio LF. Zinc as a therapy in a rat model of autism prenatally induced by valproic acid. Prog Neuropsychopharmacol Biol Psychiatry. 2018;84:173-80.
11. Lewis SA, Negelspach DC, Kaladchibachi S, Cowen SL, Fernandez F. Spontaneous alternation: A potential gateway to spatial working memory in Drosophila. Neurobiol Learn Mem. 2017;142:230-5.

12. Mageed AS, Pietryga DW, DeHeer DH, West RA. Isolation of large numbers of mesenchymal stem cells from the washings of bone marrow collection bags: characterization of fresh mesenchymal stem cells. Transplantation. 2007;83:1019-26.
13. Abdel Aziz MT, El-Asmar MF, Haidara M, Atta HM, Roshdy NK, Rashed LA, et al. Effect of bone marrow-derived mesenchymal stem cells on cardiovascular complications in diabetic rats. Med Sci Monit. 2008;140:249-55.
14. Szatanek R, Baj-Krzyworzeka M, Zimoch J, Lekka M, Siedlar M, Baran J. The methods of choice for extracellular vesicles (EVs) characterization. Int J Mol Sci. 2017;18:25-36.
15. Wu Y, Deng W, Klinke DJ, 2nd. Exosomes: improved methods to characterize their morphology, RNA content, and surface protein biomarkers. Analyst. 2015;140:6631-42.
16. Wu, Yueting, Wentao Deng, and David J. Klinke. "Exosomes: Improved Methods to Characterize Their Morphology, RNA Content, and Surface Protein Biomarkers." 2015 Analyst 140 (19): 6631–42. https://doi.org/10.1039/C5AN00688K.
17. Ma ZJ, Yang JJ, Lu YB, Liu ZY, Wang XX. Mesenchymal stem cell-derived exosomes: Toward cell-free therapeutic strategies in regenerative medicine. World J Stem Cells. 2020;12:814-40.
18. Ornoy A, Echefu B, Becker M. Valproic Acid in Pregnancy Revisited: Neurobehavioral, Biochemical and Molecular Changes Affecting the Embryo and Fetus in Humans and in Animals: A Narrative Review. Int J Mol Sci. 2023 Dec 27;25(1):390. doi: 10.3390/ijms25010390. PMID: 38203562; PMCID: PMC10779436.
19. Schneider T, Przewłocki R. Behavioral alterations in rats prenatally exposed to valproic acid: animal model of autism. Neuropsychopharmacol. 2005;30:80-9.
20. Sharma A, Mehan S. Targeting PI3K-AKT/mTOR signaling in the prevention of autism. Neurochem Int. 2021;147:105-10.
21. Huang H, Zhang G, Ge Z. lncRNA MALAT1 promotes renal fibrosis in diabetic nephropathy by targeting the miR-2355-3p/IL6ST Axis. Front Pharmacol. 2021;12:64-76.
22. Hao Y, Xie B, Fu X, Xu R, Yang Y. New insights into lncRNAs in Aβ cascade hypothesis of alzheimer's disease. Biomolecules. 2022;120:12-25.
23. Schepici G, Cavalli E, Bramanti P, Mazzon E. Autism Spectrum Disorder and miRNA: An overview of experimental models. Brain Sci. 2019;90:18-25.
24. Deng S, Zhang Y, Xu C, Ma D. MicroRNA-125b-2 overexpression represses ectodermal differentiation of mouse embryonic stem cells. Int J Mol Med. 2015 Aug;36(2):355-62. doi: 10.3892/ijmm.2015.2238. Epub 2015 Jun 8. PMID: 26059631; PMCID: PMC4501654.
25. Zhang C, Wan X, Tang S, Li K, Wang Y, Liu Y, et al. miR-125b-5p/STAT3 Pathway Regulated by mTORC1 Plays a Critical Role in Promoting Cell Proliferation and Tumor Growth. J Cancer. 2020 Jan 1;11(4):919-931. doi: 10.7150/jca.33696. PMID: 31949495; PMCID: PMC6959016.
26. Wong CW, Wang Y, Liu T, Li L, Cheung SKK, Or PM, Cheng AS, et al. Autism-associated PTEN missense mutation leads to enhanced nuclear localization and neurite outgrowth in an induced pluripotent stem cell line. FEBS J. 2020 Nov;287(22):4848-4861. doi: 10.1111/febs.15287. Epub 2020 Mar 26. PMID: 32150788; PMCID: PMC7754348.
27. Zhuang J, Cai P, Chen Z, Yang Q, Chen X, Wang X, et al. Long noncoding RNA MALAT1 and its target microRNA-125b are potential biomarkers for Alzheimer's disease management via interactions with FOXQ1, PTGS2 and CDK5. Am J Transl Res. 2020;12:5940.
28. d'Angelo M, Cimini A, Castelli V. Insights into the effects of mesenchymal stem cell-derived secretome in parkinson's disease. Int J Mol Sci. 2020;210:12-20.
29. Fričová D, Korchak JA, Zubair AC. Challenges and translational considerations of mesenchymal stem/stromal cell therapy for Parkinson's disease. NPJ Regenerative medicine. 2020;5:20-3.
30. Patel NA, Moss LD, Lee JY, Tajiri N, Acosta S, Hudson C, et al. Long noncoding RNA MALAT1 in exosomes drives regenerative function and modulates inflammation-linked networks following traumatic brain injury. J Neuroinflammation. 2018;15:204-10.